Poly(A)-Binding Protein 1 Partially Relocalizes to the Nucleus during Herpes Simplex Virus Type 1 Infection in an ICP27-Independent Manner and Does Not Inhibit Virus Replication[▽]

C. Salaun,[1]§ A. I. MacDonald,[1] O. Larralde,[1]† L. Howard,[1] K. Lochtie,[1] H. M. Burgess,[2] M. Brook,[2] P. Malik,[1]‡ N. K. Gray,[2] and S. V. Graham[1]*

Division of Infection and Immunity, Faculty of Biomedical and Life Sciences, University of Glasgow, Glasgow G12 8TT, Scotland, United Kingdom,[1] and MRC Human Reproductive Sciences Unit, Centre for Reproductive Biology, Queens Medical Research Institute, University of Edinburgh, 47 Little France Crescent, Edinburgh EH16 4TJ, Scotland, United Kingdom[2]

Infection of cells by herpes simplex virus type 1 (HSV-1) triggers host cell shutoff whereby mRNAs are degraded and cellular protein synthesis is diminished. However, virus protein translation continues because the translational apparatus in HSV-infected cells is maintained in an active state. Surprisingly, poly(A)-binding protein 1 (PABP1), a predominantly cytoplasmic protein that is required for efficient translation initiation, is partially relocated to the nucleus during HSV-1 infection. This relocalization occurred in a time-dependent manner with respect to virus infection. Since HSV-1 infection causes cell stress, we examined other cell stress inducers and found that oxidative stress similarly relocated PABP1. An examination of stress-induced kinases revealed similarities in HSV-1 infection and oxidative stress activation of JNK and p38 mitogen-activated protein (MAP) kinases. Importantly, PABP relocalization in infection was found to be independent of the viral protein ICP27. The depletion of PABP1 by small interfering RNA (siRNA) knockdown had no significant effect on viral replication or the expression of selected virus late proteins, suggesting that reduced levels of cytoplasmic PABP1 are tolerated during infection.

The lytic replication cycle of herpes simplex virus type 1 (HSV-1) can be divided into three phases, immediate-early (IE), early (E), and late (L), that occur in a coordinated sequential gene expression program. IE proteins can regulate E and L gene expression, which produces proteins involved in DNA replication, capsid production, and virion assembly. HSV infection results in host cell shutoff to facilitate the efficient production of viral proteins. First, mRNA is degraded by the virion-associated *vhs* protein, and then ICP27, a multifunctional regulator of gene expression, inhibits pre-mRNA splicing. As most viral mRNAs are intronless, this abrogates the production of stable cellular mRNAs that can be exported to the cytoplasm and compete for translation with viral mRNAs (44).

HSV mRNAs are capped and polyadenylated and so are translated via a normal cap-dependent mechanism. Translation initiation, during which translationally active ribosomes are assembled, is a tightly regulated process (21). Eukaryotic initiation factor 4F (eIF4F) (composed of eIF4E, eIF4G, and eIF4A) that binds the cap at the 5′ end of the mRNA promotes the recruitment of the 40S ribosomal subunit and associated factors, including eIF2-GTP initiator tRNA. The recognition of the start codon then promotes large ribosomal subunit joining. Poly(A)-binding protein 1 (PABP1), which binds and multimerizes on mRNA poly(A) tails, enhances translation initiation through interactions with the eIF4G component of the eIF4F cap-binding complex (20, 29, 32, 51) to circularize the mRNA in a "closed-loop" conformation (24). Key protein-RNA and protein-protein interactions in the translation initiation complex are strengthened by this PABP1-mediated circularization (12).

HSV-1 maintains active viral translation in the face of host translational shutoff. Infection activates protein kinase R (PKR), which phosphorylates eIF2α, resulting in translation inhibition. However, HSV-1 ICP34.5 redirects protein phosphatase 1α to reverse eIF2α phosphorylation, abrogating the block to translation (17, 38). In addition, the HSV-1 US11 protein inhibits PKR and may also block PKR-mediated eIF2α phosphorylation (40, 42). HSV-1 infection also enhances eIF4F assembly in quiescent cells by the phosphorylation and proteasome-mediated degradation of the eIF4E-binding protein (4E-BP), which, when hypophosphorylated, can negatively regulate eIF4F complex formation (54). However, ICP6 may also contribute to eIF4F assembly by binding to eIF4G (55). Finally, ICP6 is required for Mnk-1 phosphorylation of eIF4E, but the mechanisms behind this remain unclear (54). ICP27 has also been implicated in translation regulation during HSV infection (6, 8, 10, 30) and may also activate p38 mitogen-activated protein (MAP) kinase that can phosphorylate eIF4E (16, 59).

* Corresponding author. Mailing address: Division of Infection and Immunity, Faculty of Biomedical and Life Sciences, University of Glasgow, Glasgow G12 8TT, Scotland, United Kingdom. Phone: 44 141 330 6526. Fax: 44 141 330 4600. E-mail: s.v.graham@bio.gla.ac.uk.
† Present address: Transfusion Transmitted Infection Group, Research & Development Directorate, Scottish National Blood Transfusion Service, 21 Ellen's Glen Road, Edinburgh EH17 7QT, United Kingdom.
‡ Present address: Institute of Cell Biology, Michael Swann Building, King's Buildings, University of Edinburgh, Mayfield Road, Edinburgh EH9 3JR, Scotland, United Kingdom.
§ Present address: Centre de Recherche, INSERM U845, Université Paris Descartes, Faculté de Médecine, 156 Rue de Vaugirard, F-75015 Paris, France.
▽ Published ahead of print on 23 June 2010.

PABP1 appears to be a common cellular target of RNA and DNA viruses. PABP1 can undergo proteolysis, intracellular relocalization, or modification of its interaction with other translation factors in response to infection. For example, poliovirus induces host cell shutoff by cleaving PABP1, thus disrupting certain PABP1-containing complexes (28, 29). The rotavirus NSP3 protein can displace PABP1 from translation initiation complexes (41). However, NSP3 also interacts with a cellular protein, RoXaN, which is required to relocate PABP1 to the nucleus (13). Similarly, the Kaposi's sarcoma herpesvirus (KSHV) SOX protein plays a role in relocating PABP1, its cofactor in cellular mRNA decay, to the nucleus (33). Although steady-state levels of PABP1 are highest in the cytoplasm of normal cells, where it has cytoplasmic functions, it is a nucleocytoplasmic shuttling protein (1). However, it is unclear how PABP1 enters or exits the nucleus, as it contains neither a canonical nuclear export nor an import signal.

Here we describe the loss of PABP1 from cap-binding complexes and the partial relocation of PABP1 to the nucleus in HSV-1-infected cells in a time-dependent manner. Relocation is specific for PABP1, as other translation factors remained in the cytoplasm. Cells undergo stress during HSV-1 infection, and analysis of a variety of cell stresses revealed that PABP relocalization was also observed upon oxidative stress. Paxillin, a potential PABP1 nuclear chaperone, was phosphorylated, and the paxillin-PABP1 interaction was reduced during virus infection. However, the interaction was weak and cell type dependent, indicating that other effectors of PABP1 relocation in the infected cell must exist. Recently, the HSV-1 ICP27 protein was suggested to alter the PABP1 cellular location (6). However, infections with ICP27-null mutant viruses clearly demonstrated that ICP27 is not required for PABP1 nuclear relocation in the context of infection. Although HSV-1 mRNAs are translated by a normal cap-dependent mechanism known to be enhanced by PABP1, small interfering RNA (siRNA) knockdown of PABP1 indicated that at late times of infection, the translation of certain virus late proteins tolerates very low levels of PABP1.

MATERIALS AND METHODS

Cells and viruses. HeLa and Vero cells were grown to subconfluence in Dulbecco's modified Eagles medium (DMEM; Invitrogen) with 10% fetal calf serum, 50 µg/ml penicillin, and 50 µg/ml streptomycin at 37°C in 5% CO_2. Cells were infected with HSV-1 wild-type strain KOS1.1 or the HSV-1 ICP27-null mutant virus 27lacZ, where the ICP27 gene is inactivated by the insertion of a *lacZ* gene cassette (49), or the ICP27-null virus d27-1, where the ICP27 promoter and most of the gene coding sequence have been deleted (43). Virus was adsorbed onto cells for 1 h. Viruses were used at a range of multiplicities of infection (MOIs) (0.1, 1, 5, and 10) as detailed in the figure legends. Wild-type virus replication was assessed by titration on BHK-1 cells.

Cell lysis and fractionation. For coimmunoprecipitation experiments, total cellular protein lysates were obtained by scraping cells into NP-40 lysis buffer (150 mM NaCl, 50 mM Tris [pH 8.0], 2 mM EDTA, complete miniprotease inhibitor cocktail mix and complete phosphoSTOP [Roche Diagnostics], and 0.5% NP-40) and pelleting debris by centrifugation at $10,000 \times g$ for 5 min in an Eppendorf microcentrifuge. For Western blot analysis cells were scraped into 2× SDS-polyacrylamide gel loading buffer. DNA was sheared by 10 passes through an 18-gauge needle and sonication for 30 s in a Sonibath (Kelly Electronics). Membrane, cytosol, and nuclear cell fractions were prepared by using a Biovision FractionPREP cell fractionation kit according to the manufacturer's instructions (Biovision, CA). Cell numbers were counted, and cell equivalents of total cell protein or of the various fractions were compared on SDS-PAGE gels.

Western blot analysis. Proteins were fractionated on 4 to 12% gradient SDS-polyacrylamide gel electrophoresis gels (NuPage; Invitrogen) and transferred onto a nitrocellulose membrane by using an I-Blot dry blotting system (Invitrogen). Membranes were blocked in 5% milk powder in phosphate-buffered saline (PBS) containing 0.1% Triton X-100 (PBST) for 1 h with shaking. Membranes were incubated with primary antibodies diluted in 5% milk powder in PBST overnight at 4°C, and following washing in PBST, they were incubated with secondary antibody (anti-mouse IgG or anti-rabbit IgG, diluted at 1:2,000 [ECL; GE Healthcare]) for 1 h with shaking. Following washing in PBST, proteins were visualized by using ECL Western blotting detection reagent (Pierce, Thermo Scientific). Monoclonal primary antibodies used were those against PABP1 (10E10), ICP4, ICP8, gC (all Abcam), ICP27 (1119/1113; Virusys Corporation), S6 ribosomal protein (Cell Signaling Technology), glyceraldehyde-3-phosphate dehydrogenase (GAPDH) (6CS; Biodesign), and SRp20 (7B4; Zymed laboratories), all used at a 1:1,000 dilution. Other monoclonal antibodies were eIF4E (1:500) and paxillin (1:10,000) (BD Transduction Laboratories) and VP16 (1:500; Santa Cruz). Polyclonal antibodies used were those against PABP1 (1:5,000; Abcam) and PABP1 C terminus polyclonal antibody RED2 (1:5,000; a gift from Simon Morley, University of Sussex), p53 CM-1 (1:1,000; Leica), and connexin 43 (1:1,000; Sigma).

Confocal microscopy. A total of 8×10^4 cells per coverslip were grown overnight on sterile 18- by 18-mm coverslips and then infected or mock infected with virus for the required time period. Cells on coverslips were washed three times with PBS and fixed in 20% sucrose–5% formaldehyde in PBS for 10 min at room temperature. After three washes with PBS, the coverslips were permeabilized with a 70% acetone–30% methanol solution for 5 min at −20°C and then washed three times with PBS and incubated in PBS containing 20% calf serum for 1 h at room temperature. Cells were incubated with primary antibodies diluted in 1% calf serum in PBS for 1 h at room temperature: ICP27 (1119/1113, 1:100; Virusys Corporation), ICP4 (1:200; Abcam), PABP1 (10E10; Abcam), RED2 (1:300; a gift from Simon Morley, University of Sussex), paxillin (1:250; BD Transduction Laboratories), eIF3 (1:100; Santa Cruz), and eIF4E (1:500; Abcam). Coverslips were washed in PBS six times before incubation for 1 h with Alexa Fluor 350, 488, 555, or 647 donkey anti-mouse secondary antibody or Alexa Fluor 488 or 555 donkey anti-rabbit antibody diluted 1:1,000 in 1% (vol/vol) calf serum in PBS (Vector Laboratories). After washing in PBS six times, coverslips were mounted with Vectashield mounting medium (with DAPI [4′,6-diamidino-2-phenylindole] as a nuclear stain). Images were taken by using a Zeiss LSM510 Meta confocal microscope.

Coimmunoprecipitation. Cell lysates (500 µg) were RNase treated (5 µg) prior to use by incubation for 1 h at 37°C. For immunoprecipitation, protein G beads (Sigma) were washed three times in NP-40 lysis buffer. Beads were used to preclear lysates by incubation for 1 h at 4°C with rotation. Supernatants were incubated with 1 µg polyclonal antibody (PAIP2, SRPK1 [Santa Cruz], and paxillin [Abcam]) for 1 h at 4°C before the addition of fresh, washed protein G beads (50-µl slurry) and overnight incubation at 4°C. Beads were pelleted and washed five times with NP-40 lysis buffer. After a final wash, beads were suspended in SDS-PAGE loading buffer and boiled for 5 min. Beads were pelleted by a brief centrifugation, and supernatants were analyzed by SDS-PAGE.

Irradiation and drug treatment of cells. HeLa cells were seeded at 10^5 cells per well in 24-well culture dishes containing sterile coverslips. Cells were allowed to settle for 24 h at 37°C. Medium was removed, and cells were irradiated by using a gamma irradiation cobalt^{60} source (0.5 to 20 Gy). Fresh medium was added to each well, and cells were placed into a CO_2 incubator overnight at 37°C. A range of concentrations and a range of times of incubation with tunicamycin, thapsigargin (dissolved in dimethyl sulfoxide [DMSO]), and H_2O_2 (dissolved or diluted in H_2O) were also tested. The final concentration and dosage time of each drug used were the highest that did not cause apoptosis, as noted in the figure legends in each case. Drugs were added to media prior to being added to cells. Controls were cells treated with drug vehicle alone.

Transient transfection and siRNA knockdown. For the ectopic expression of ICP27, HeLa cells on coverslips in 24-well dishes were transiently transfected with 0.1 µg per well of plasmid pEGFP-C1, encoding ICP27, by using Attractene (Qiagen). The medium was replaced after 24 h. Cells were fixed 48 h after transfection and processed for confocal immunofluorescence microscopy. For siRNA knockdown, a pool of three siRNA duplexes that target PABP1 RNA was purchased from Santa Cruz. Cells were transfected at 50% confluence in six-well dishes with 10 nM siRNA using Lipofectamine RNAiMax (Invitrogen) diluted in Opti-MEM (Invitrogen). Fresh medium without antibiotics was added to each well and incubated at 37°C in 5% CO_2 for 24 h. Cells were infected with HSV-1 at an MOI of 5 and harvested 16 h postinfection. For virus titration, plates were frozen at −80°C, and detached cells were harvested and sonicated for 30 s in a Sonibath (Kelly Electronics). Virus was titrated on BHK-21 cells at 90% confluence.
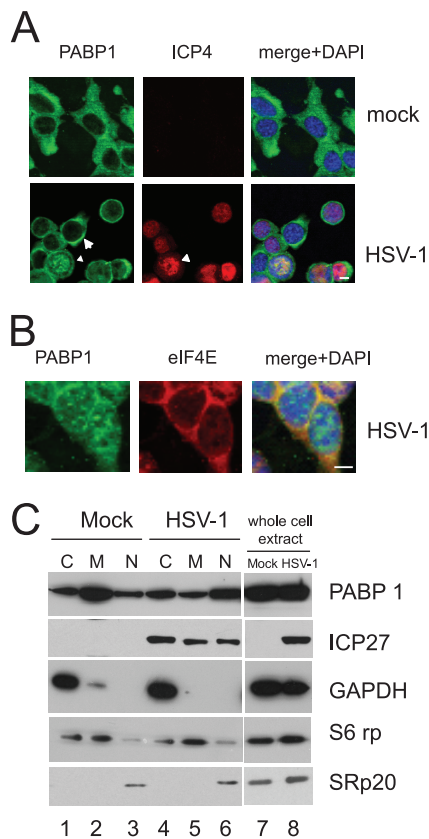
FIG. 1. Confocal microscopy analysis of PABP1 location during HSV-1 infection. (A) Immunofluorescence microscopy images of the PABP1 (green) location in mock-infected (mock) and wild-type HSV-1-infected (HSV-1) HeLa cells. A multiplicity of infection of 1 was used in each case of virus infection, and cells were examined at 9 h postinfection. Costaining with ICP4 (red) was used to monitor virus infection and to mark virus replication centers. Cells were counterstained with DAPI (blue) to locate nuclei. Arrowheads indicate a cell where PABP1 has moved to the nucleus and replication centers are forming. An arrow indicates an uninfected cell with cytoplasmic PABP1. (B) Cells infected with wild-type HSV-1 were reacted with PABP1 antibody (green) or an antibody against the translation factor eIF4E (red) and then examined by confocal microscopy. Cells were counterstained with DAPI (blue) to locate nuclei. Bar, 10 μm. (C) Western blot analysis of relative levels of PABP1 in cytoplasmic (C), membrane (M), and nuclear (N) fractions of HeLa cells either mock infected (Mock) or infected with wild-type HSV-1 at a multiplicity of infection of 5 for 9 h. S6 rp, S6 ribosomal protein, a marker of the ribosome location in cytoplasmic and membrane fractions. GAPDH is a marker of cytoplasmic fractions. SRp20 is a marker of nuclear fractions. ICP27 marks virus-infected extracts.

RESULTS

PABP1 subcellular distribution changes during HSV-1 infection. PABP1 enhances translation efficiency and is emerging as a viral target, contributing, in some cases, to host shutoff during infection (3, 13, 53). To investigate any effect of HSV-1 infection on PABP1, we analyzed PABP1 levels and subcellular localization in mock-infected and HSV-1-infected HeLa cells. In the experiment shown in Fig. 1A, a multiplicity of infection of 1 was used in order to be able to visualize uninfected cells adjacent to infected cells. PABP1 was predominantly cytoplasmic in mock-infected cells. A very similar pic-

ture was observed with cells infected for 6 h (Fig. 2 and data not shown). However, at 9 h (Fig. 1A) and 12 h (Fig. 2 and data not shown) postinfection, PABP1 levels were increased in the nuclei of the subpopulation of cells that displayed features consistent with late events in the virus replication cycle. For example, these cells displayed replication centers that stained positive for the virus transcription factor ICP4 (Fig. 1A), and cells appeared rounded up, indicative of late ongoing infection. Relocation of PABP1 was not observed for cells that did not express ICP4 (Fig. 1A). Relocalization was observed at a range of multiplicities of infection (0.1, 1, and 10) and was specific to PABP1, as other proteins involved in translation, eIF4E (Fig. 1B) and eIF3 (data not shown), remained in the cytoplasm until cells showed evidence of apoptosis. PABP1 relocalization was also observed for Vero cells (Fig. 2 and see Fig. 4A and Table 1), showing that it was not cell type specific. PABP1 relocalization was only partial, as some cytoplasmic PABP1 could be observed even at 16 h postinfection (Fig. 1B).

Biochemical subcellular fractionation experiments were carried out to confirm the confocal immunofluorescence data. Total cellular protein and cytosol, membrane, and nuclear fractions were prepared (Fig. 1C). Analysis of whole-cell extracts indicated that total PABP1 levels were not changed after 9 h of infection. The purity of the nuclear fraction was demonstrated by Western blotting with an antibody against SRp20, a splicing factor that is mainly nuclear at steady state (Fig. 1C, lanes 3 and 6). As a marker for the translation apparatus, we used the S6 ribosomal protein. The S6 ribosomal protein was found mainly in the membrane and cytosolic fractions (Fig. 1C, lanes 1, 2, 4, and 5). This is because there are two types of ribosomes, "free" ribosomes located in the cytosol and membrane-bound, endoplasmic reticulum (ER)-associated ribosomes. A trace of S6 ribosomal protein was detected in the nuclear fraction. This is likely due to polyribosomes being attached to the nuclear membrane. The S6 ribosomal protein acts as a control for the location of ribosome-associated PABP1. GAPDH was found mainly in the cytosolic fraction (Fig. 1C, lanes 1 and 4), as expected. There was little difference in the subcellular locations of the control proteins between mock-infected and HSV-1-infected cells. However, PABP1 was clearly partially redistributed in HSV-1-infected cells. In mock-infected cells PABP1 was found mainly in the membrane fraction (Fig. 1C, lane 2), with some located in the cytoplasm, similar to the location of the S6 ribosomal protein. PABP1 was also found in the nucleus, as expected, as it has nuclear functions (11). In contrast, in HSV-1-infected cells, although PABP1 was still present in the cytosol (Fig. 1C, lane 4), levels were reduced in the membrane fraction (Fig. 1C, lane 5) but increased in the nuclear fraction (Fig. 1C, lane 6). HSV-1 infection did not change the subcellular location of the S6 ribosomal protein, indicating that changes in PABP1 location are not due to a general disruption of the translation apparatus. There may appear to be a greater relocation of PABP1 to the nucleus in this experiment compared to the confocal data shown in Fig. 1A due to the increased multiplicity of infection of 5 used in this biochemical fractionation experiment.

PABP1 is relocated during HSV-1 infection in a time-dependent manner. HeLa and Vero cells were infected for 3, 6, 9, and 12 h with HSV-1 at a multiplicity of infection of 1. Confocal microscopy was used to examine the PABP1 location at
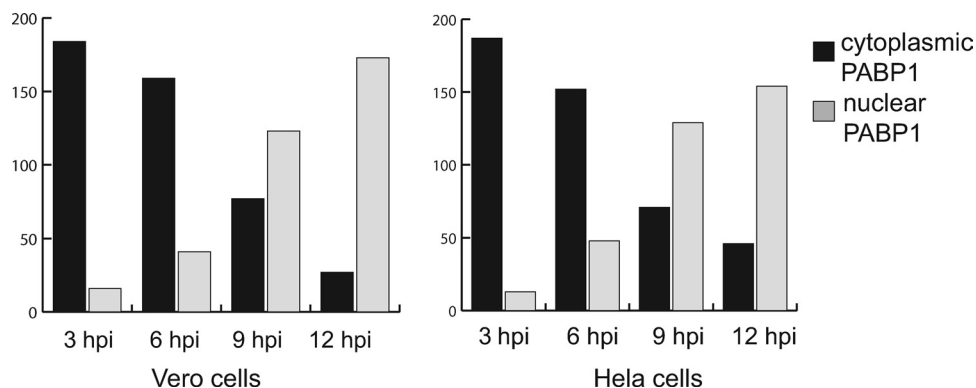
FIG. 2. PABP1 relocates to the nucleus in wild-type HSV-1-infected Vero and HeLa cells in a time-dependent manner. HeLa and Vero cells on coverslips were infected at a multiplicity of infection of 1 with wild-type HSV-1, and coverslips were harvested at 3, 6, 9, and 12 h postinfection (hpi). For each time point, ICP4-positive cells were counted (200 cells in each case). Patterns of staining were categorized into PABP1 location mainly in the cytoplasm (cytoplasmic PABP1) (black bars) or mainly in the nucleus (nuclear PABP1) (gray bars). Dividing cells and cells that had similar levels of PABP1 present in both compartments (less than 10% of the total cell population) were not counted. Two separate experiments for each cell line were carried out, with very similar results. Data from one such experiment are shown.

each infection time point. Cells that showed expression of ICP4 were counted for each time point (200 cells). Two separate experiments for each cell line were carried out, with very similar results. Data from one experiment are shown. The number of cells that displayed predominantly nuclear PABP1 increased with time postinfection, with the majority of cells (~70%) containing some nuclear PABP1 by 12 h postinfection (Fig. 2).

Oxidative stress causes relocalization of PABP1 to the nucleus. HSV infection leads to JNK and p38 MAP kinase activation (11, 16, 59). JNK and p38 MAP kinase activation is also a common feature of cell stress. Cells frequently respond to stress by downregulating global translation (50). Some inducers of cell stress cause PABP1 localization to cytoplasmic stress granules. However, the loss of PABP1 from the cytoplasm to the nucleus at late times of HSV-1 infection could be a different response to cell stress linked to the virus-induced stress response. Figure 3A confirms that most JNK and p38 MAP kinases were robustly activated during HSV-1 infection. This suggests that PABP1 nuclear relocalization may also occur following other cell stresses where PABP1 is not relocalized to

TABLE 1. Occupancy of PABP1 in HSV-1 infected cells[a]

Time postinfection (h)	Mean % occupancy of PABP1 ± SEM			
	Vero cells		HeLa cells	
	Cytoplasm	Nucleus	Cytoplasm	Nucleus
6	68.3 ± 8.2	11.1 ± 3.1	74.5 ± 6.9	13.2 ± 2.5
16	11.2 ± 4.2	67.7 ± 13.8	7.2 ± 1.9	50.7 ± 10.4

[a] Cells on coverslips at a confluence of 70% were infected with HSV-1 at a multiplicity of infection of 1. At either 6 or 16 h postinfection, cells were fixed onto coverslips by incubation in 20% sucrose–5% formaldehyde in PBS for 10 min at room temperature. Antibody staining and immunofluorescence confocal microscopy were carried out with a Zeiss LSM 500 confocal microscope. Cell pictures were counted blind by two individuals. Cells showing evidence of virus infection by the detection of ICP4 expression from images from three different experiments (500 cells for each experiment) were counted in each case. Only nondividing cells were counted. Cells where there was a significantly higher level of PABP1 in the nucleus than in the cytoplasm were counted as having nuclear PABP1. Around 5 to 10% of cells showed similar levels of PABP1 in the nucleus and cytoplasm, and these cells were not counted.

stress granules. Therefore, uninfected cells were stressed by various means, including gamma irradiation-induced DNA damage, ER and oxidative stress, and the location of PABP1 was examined by confocal microscopy. We tested a range of drug concentrations and radiation doses. Experiments were carried out under conditions where full apoptosis was not observed, as judged by evidence of fragmentation of DAPI-stained DNA and cell detachment from culture flasks. Changes in PABP1 location were not observed in most cases, including gamma irradiation of cells (Fig. 3C). However, treating cells with inducers of oxidative stress caused changes in PABP1 subcellular localization. PABP1 relocated to the nucleus following 2 h of treatment with between 500 and 1,000 μM hydrogen peroxide (Fig. 3D). Although quantitative differences were observed, qualitatively, the hydrogen peroxide activation of stress kinases had a profile similar to that seen with HSV-1 infection (Fig. 3B). In particular, both treatments of Vero cells resulted in a significant activation of JNK2 and p38α MAP kinases (Fig. 3A and B). As HSV-1 infection and hydrogen peroxide cause ER stress (34, 37, 52), we also investigated whether ER stress results in the relocation of PABP1. The effect of known inducers of ER stress, tunicamycin (10 μg/ml) (Fig. 3E) or thapsigargin (2 μM) (data not shown), was tested on HeLa cells. Neither drug induced PABP1 relocation at concentrations known to induce ER stress. The incubation of cells with drug vehicle alone also did not cause relocation in any case (e.g., see Fig. 3F). HSV-1 infection is known to induce oxidative stress (26). We suggest that PABP1 subcellular relocation during HSV-1 infection may be a direct and selective response to virus-induced oxidative stress.

Paxillin may contribute to PABP1 relocalization to the nucleus. The cell attachment, spreading, and motility regulator protein paxillin has been shown to interact directly with PABP1, and it was previously suggested to contribute to PABP1 export from the nucleus (57, 58). Thus, changes to paxillin in HSV-1-infected cells could cause a redistribution of PABP1 to the nucleus. Paxillin is found at focal adhesions at the leading edge of migrating cells (5) but is also located to the perinuclear endoplasmic reticulum (58). In uninfected Vero
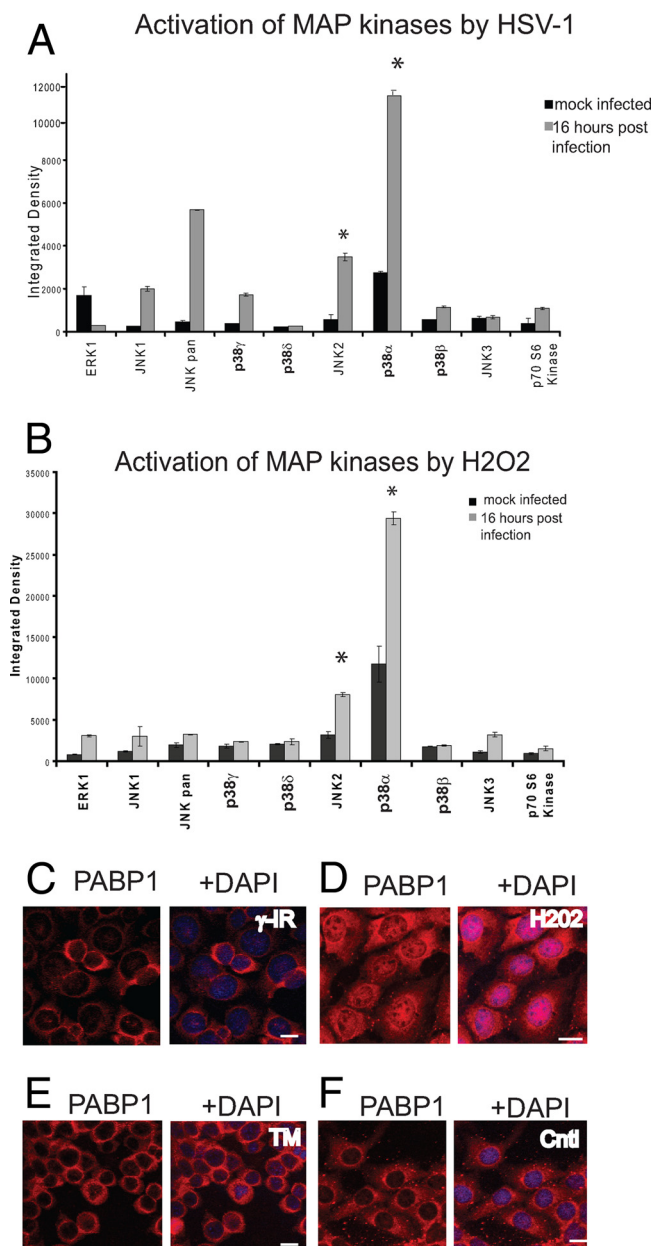
FIG. 3. Oxidative stress induces PABP1 relocation to the nucleus. (A) Relative levels of activated, selected signaling MAP kinases in mock-infected (black bars) and HSV-1-infected (dark gray bars) Vero cells (16 h postinfection at a multiplicity of infection of 5) assessed by using the Proteome Profiler Array human phospho-MAPK array kit (R&D Systems, Minneapolis, MN) according to the manufacturer's instructions. (B) Relative levels of activated, selected signaling MAP kinases in mock-treated (black bars) and hydrogen peroxide-treated (1,000 μM for 2 h at 37°C) (light gray bars) Vero cells assessed using the same array kit as that described for panel A. The graphs show the means and standard errors of the means from three separate experiments, although standard errors of the means were very low, and error bars lie very close to the tops of the bars on the graphs. Asterisks indicate JNK and p38 MAP kinases whose activities increased significantly upon both HSV-1 infection and hydrogen peroxide treatment. (C to F) Confocal immunofluorescence microscopy analysis of the effects of irradiation, or selected drug treatments, on PABP1 location in uninfected HeLa cells. (C) Gamma irradiation (γ-IR) does not alter the subcellular location of PABP1. Irradiation was tested between 0.5 and 20 Gy. The image shows cells irradiated to 20 Gy and incubated

cells, paxillin showed a diffuse cytoplasmic location (Fig. 4A). Very few focal adhesions were observed, but paxillin localized to any that were present (data not shown). In HSV-1-infected Vero cells, paxillin was also found in the cytoplasm but had a more perinuclear location. However, in infected Vero cells, although some PABP1 was present in the same perinuclear location as paxillin, a significant portion relocated to the nucleus (Fig. 4A). Paxillin phosphorylation regulates its subcellular localization (7), and the paxillin that interacts with and exports nuclear PABP1 was previously reported to be hypophosphorylated (57). Thus, the hyperphosphorylation of paxillin could induce a nuclear accumulation of PABP1 by causing paxillin to remain in the cytoplasm or by inhibiting the formation of exportable nuclear PABP1-paxillin complexes. A comparison of the paxillin protein from mock-infected and HSV-1-infected Vero cells showed that HSV-1 infection induced significant changes in the mobility of paxillin on SDS-PAGE gels (Fig. 4B). The treatment of total cell extracts from mock- and HSV-1-infected cells with calf intestinal alkaline phosphatase indicated that the decreased mobility of paxillin isolated from HSV-1-infected cells was due to changes in phosphorylation (Fig. 4C). To assess the formation of PABP1-paxillin complexes, coimmunoprecipitation was carried out on mock-infected and infected cell extracts. A small amount of paxillin was found in complex with PABP1 in mock-infected Vero cells, but no paxillin-PABP1 interaction could be demonstrated for HSV-1-infected Vero cells (Fig. 4D). Paxillin was present in infected cell lysates and could be precipitated with the anti-paxillin antibody used. PAIP2, a binding partner of PABP1 (27), could efficiently precipitate PABP1 from mock-infected or HSV-1-infected Vero cell extracts (Fig. 4E). No coimmunoprecipitation was observed with the control antibody, SR protein kinase 1 (SRPK1), which is involved in RNA metabolism but has not been reported to bind paxillin or PAIP2. Our finding that the PABP1-paxillin interaction in uninfected cells was hard to detect casts doubt over the extent to which the observed loss of this interaction might contribute to PABP1 relocalization in Vero cells. Indeed, PABP1-paxillin interactions were unable to be detected in HeLa cells (data not shown) where PABP1 is also relocated to the nucleus, suggesting that this interaction is highly unlikely to account for the nuclear accumulation of PABP1 during HSV-1 infection.

ICP27 is not required for PABP1 relocation to the nucleus during HSV-1 infection. Recently, it was reported that the ectopic expression of the HSV-1 protein ICP27 caused increased nuclear levels of PABP1 (6). We confirmed that the ectopic overexpression of green fluorescent protein (GFP)-labeled ICP27 results in the relocation of PABP1 to the nucleus (Fig. 5A). To explore whether ICP27 also causes PABP1 relocation during HSV-1 infection, HeLa cells were infected

overnight at 37°C. (D) Oxidative stress was induced with 1,000 μM hydrogen peroxide (H₂O₂) and incubation for 2 h at 37°C, with significant PABP relocation to the nucleus. (E) ER stress does not cause PABP1 relocation to the nucleus. ER stress was induced by the treatment of cells with 10 μg/ml tunicamycin (TM) for 8 h at 37°C. (F) Mock-treated cells (control [cntl]). Significant levels of cell death were not observed under any of the conditions used. Bar, 10 μm.
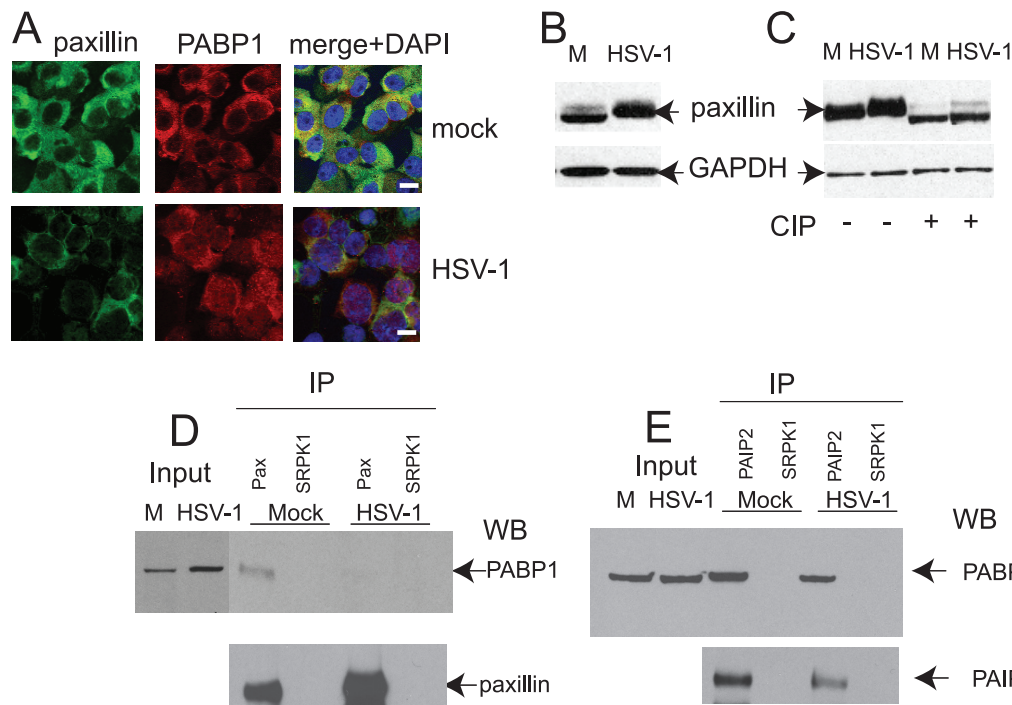
FIG. 4. The interaction of paxillin with PABP1 is disrupted in HSV-1-infected Vero cells. (A) Immunofluorescence microscopy analysis of the subcellular locations of paxillin (green) and PABP1 (red) in mock-infected (mock) and HSV-1-infected (HSV-1) Vero cells. Infection was carried out at a multiplicity of infection of 5 for 9 h. DNA in the nuclei is counterstained with DAPI (blue). (B) Western blot analysis of the mobility of the paxillin protein from mock-infected (M) and HSV-1-infected (HSV-1) Vero cells on SDS-PAGE gels. The lower portion of the Western blot was probed with GAPDH antibody to demonstrate equal protein loading. (C) Calf intestinal alkaline phosphatase (CIP) at 1 U/μg protein was added to protein lysates and incubated for 1 h at 37°C. Proteins were fractionated on SDS-PAGE gels and Western blotted with an anti-paxillin antibody or a GAPDH antibody control. M, mock-infected cell lysate; HSV-1, HSV-1-infected cell lysate. (D and E) Coimmunoprecipitation of PABP1 from mock-infected or HSV-1-infected Vero cells with paxillin (D) and PAIP2 (E), a known PABP1-interacting protein (27). (Top) Western blot (WB) analysis of immunoprecipitation (IP) of PAIP2- or paxillin-containing complexes fractionated by SDS-PAGE and Western blotted with PABP1 antibody. (Bottom) Results of Western blotting of the coimmunoprecipitated complexes with the cognate antibody. Pax, paxillin antibody used in coimmunoprecipitation; PAIP2, PAIP2 antibody used in coimmunoprecipitation; SRPK1, SRPK1 antibody used as a control antibody; M, mock-infected cell lysate; HSV-1, HSV-1-infected cell lysate. Input lanes contained 10% of the quantity of cell lysate used in the coimmunoprecipitation experiments.

with the ICP27 mutant virus 27lacZ, where the ICP27 gene is disrupted by the insertion of a *lacZ* gene. If ICP27 was involved in PABP1 relocation, then no relocation should be observed for cells infected with the ICP27-null mutant virus. Figure 5B shows that in cells infected with HSV-1 27lacZ (arrowed cells), PABP1 relocated to the nucleus in a manner similar to that observed for cells infected with wild-type HSV-1 (Fig. 1A). A very similar result was obtained when cells were infected with d27.1, an ICP27 deletion mutant virus (data not shown). Cells infected with the ICP27 mutant viruses did not become rounded up, and replication centers were not as well formed as in the cells infected with wild-type virus, as expected. This is because ICP27 is required for efficient virus DNA replication, and infection proceeds more slowly with ICP27 mutant viruses (35). However, in cells where replication centers were beginning to form (ICP4-positive cells), PABP1 clearly relocated to the nucleus. Quantification of numbers of cells with mainly cytoplasmic versus mainly nuclear PABP1 demonstrated a similar time-dependent relocation of PABP1 to the nucleus, although the numbers of cells with predominantly cytoplasmic PABP1 did not fall as low as those in wild-type HSV-1-infected cells, again likely due to differences in the course of infection with ICP27 mutant viruses (Fig. 5C).

Reduction in PABP1 levels does not affect progression of HSV-1 infection or synthesis of virus late proteins. HSV-1 replicates in the nucleus, and virus mRNAs are capped and polyadenylated, like cellular mRNAs. Therefore, the efficient translation of viral mRNAs requires an active cellular translation machinery. Decreased PABP1 levels in the cytoplasm at late times of virus infection would be predicted to have a negative impact on virus translation and replication. The level of PABP1 associated with cap-binding complexes was shown to be decreased in HSV-1-infected cells (6). Since HSV-1 mRNAs are capped and polyadenylated, the loss of PABP1 from the translational apparatus would be predicted to be detrimental to HSV-1 translation and replication. However, our observations suggest that the loss of PABP1 may be tolerated.

To test whether virus replication was altered by the absence of PABP1, siRNA knockdown was performed. A pool of PABP1-specific siRNAs knocked down PABP1 by around 90% over a 24-h period (Fig. 6A). Cells were treated with siRNA for 72 h prior to infection with HSV-1 at a multiplicity of infection of 0.1. At 24 h following infection, virus replication was measured by determining virus titers. No significant difference in virus replication was noted for HSV-1-infected HeLa cells
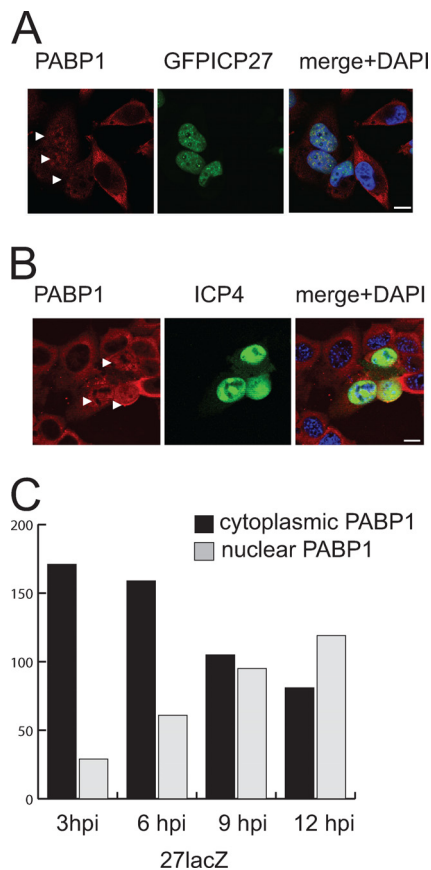
FIG. 5. ICP27 does not cause PABP1 relocation to the nucleus during HSV-1 infection. (A) HeLa cells were transiently transfected with a plasmid encoding GFP-tagged ICP27 and 48 h later examined for ICP27 expression (green) and PABP1 localization (red) by immunofluorescence confocal microscopy. Nuclei were counterstained with DAPI (blue). Arrowheads indicate cells where PABP1 is found in the nucleus. Bar, 10 μm. (B) HeLa cells were infected with HSV-1 ICP27 mutant virus 27lacZ at a multiplicity of infection of 1 and examined 9 h postinfection by confocal immunofluorescence microscopy. Arrowheads indicate cells where PABP1 (red) has relocated to the nucleus. Cells were also stained with antibody against ICP4 (green) to mark prereplication centers and counterstained with DAPI to locate nuclei. (C) Graph showing the distribution of PABP1 in HeLa cells infected with 27lacZ at a multiplicity of infection of 1 for various times. Very similar data were obtained with infections of Vero cells. Cell growth, analysis, and counting were exactly as detailed in the legend to Fig. 2. Two separate experiments were carried out, with very similar results. Data from one such experiment are shown.
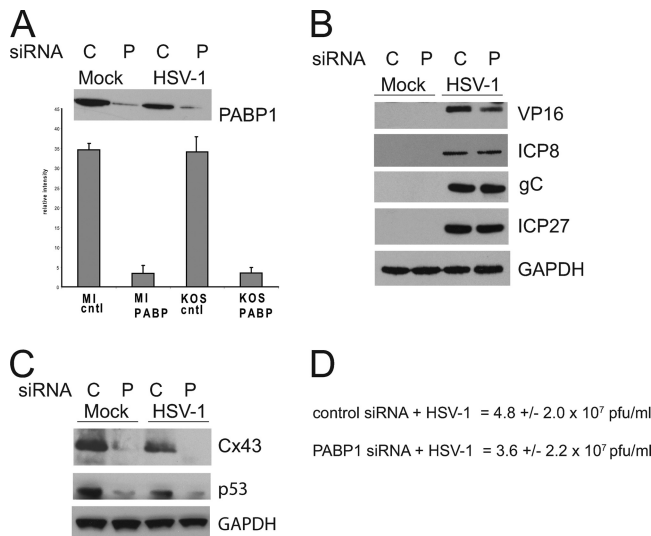

FIG. 6. Reduced levels of PABP1 in cap-binding complexes do not compromise virus replication or translation of selected viral proteins. (A) Western blot panel showing levels of PABP1 in mock- and HSV-1-infected cells treated with control siRNA (C) or PABP1 siRNA (P) for 24 h. The graph shows the means and standard errors of the means from quantifications, using Image J, of the band intensity relative to that of GAPDH controls from four separate experiments. (B) Cell lysates were prepared from HeLa cells that were first transfected with control siRNAs (C) or PABP1 siRNAs (P) for 24 h and then either mock infected (mock) or infected with HSV-1 (HSV-1) for 16 h at a multiplicity of infection of 5. Proteins were fractionated on SDS-PAGE gels and Western blotted with the antibodies against cellular and viral proteins shown on the right-hand side. (C) The same cell lysates used as described for panel B were fractionated on SDS-PAGE gels and Western blotted with the antibodies against connexin 43 (Cx43) and p53. (D) HeLa cells were transfected with control siRNAs or with PABP1 siRNAs for 72 h and then infected with HSV-1 at a multiplicity of infection of 0.1 for 24 h. Virus was titrated on BHK cells, and the titer was measured in PFU/ml. The means and standard errors of the means from four experiments are shown.

pretreated with PABP1 siRNAs compared to cells pretreated with control siRNA (Fig. 6D). Western blotting was used to examine whether a reduction in PABP1 levels altered viral protein synthesis. We did not examine ongoing translation in infected cells using metabolic labeling because siRNA knockdown of PABP1 was achieved prior to virus infection, so any effect on virus protein production should be observed at steady-state protein levels. Moreover, metabolic labeling following PABP knockdown could not be used to measure host protein synthesis because host shutoff means that very little host mRNA translation is occurring late in virus infection. Figure 6B shows data for virus protein production in cells treated with control or PABP1 siRNAs for 24 h and then either

mock infected or infected with HSV-1 for 16 h. Levels of ICP27, an immediate-early protein; ICP8, an early protein; and VP16 and gC, both true late proteins, were examined by Western blotting. No significant difference in protein levels was detected following HSV-1 infection of cells pretreated with control siRNAs or with PABP1 siRNAs (Fig. 6B), although a slight reduction in VP16 levels was observed for HSV-1-infected, PABP1 siRNA-pretreated cells. Metabolic labeling indicated a reduction of 78% in host translation in uninfected cells upon treatment with PABP1 siRNA. To discover whether PABP1 knockdown had any effect on host cell mRNA translation during virus infection, we chose to examine steady-state levels of two proteins with short half-lives (Fig. 6C). Following PABP1 knockdown, proteins already synthesized will remain detectable in the cell by Western blotting if they have long half-lives, i.e., they are not degraded during the experiment (for example, GAPDH), or efficient translation of their mRNAs is not PABP1 dependent. Conversely, levels of proteins with very short half-lives should be depleted at steady-state levels upon PABP1 siRNA treatment. Connexin 43 (Cx43) is a gap junction protein found at the membrane and in the cytoplasm and has a half-life of 1.5 to 2 h. p53 is a nuclear protein with a half-life of approximately 30 min. Levels of both

proteins were reduced in uninfected and infected cells treated with PABP1 siRNA compared to cells treated with control siRNA. In control siRNA-treated, HSV-1-infected cells, levels of the two proteins were detected but at somewhat reduced levels. Cx43 was undetected in HSV-1-infected PABP1 knockdown cells, while p53 was still able to be detected. This lack of a complete depletion of p53 during infection may be related to the previously observed virus stabilization of p53 (4). These data indicate that PABP siRNA treatment of cells can inhibit protein synthesis but that HSV-1 replication can proceed efficiently even in the presence of reduced levels of PABP1 and that at least some virus proteins are still able to be translated to normal levels.

DISCUSSION

Although mainly cytoplasmic at steady state, PABP1 can be found in the nucleus during infection with certain viruses, including rotavirus (13) and Kaposi's sarcoma herpesvirus (KSHV) (2, 33). Herpesviruses replicate in the nucleus, where the cellular RNA processing machinery adds 5′ caps and 3′ poly(A) tails to viral mRNAs. Thus, herpesvirus mRNAs mimic cellular mRNAs during translation. Like other viruses, it is possible that the reorganization of the translation apparatus ensures the preferential translation of viral mRNAs (48). The role of PABP1 in enhancing the translation of capped and polyadenylated mRNAs prompted an investigation of the effect of HSV-1 infection on PABP1 during the course of HSV-1 infection. Confocal microscopy and biochemical fractionation demonstrated a significant time-dependent accumulation of PABP1 in the nuclei of cells beginning after 6 h postinfection with wild-type HSV-1, consistent with a reduction in levels of PABP1 in cap-binding complexes. However, a complete relocation of PABP to the nucleus at late times of virus infection did not occur even at very late times of infection in cells with fully formed replication centers.

During the preparation of the manuscript, another laboratory reported that the ectopic overexpression of ICP27 caused a relocation of PABP1 to the nucleus, and those researchers concluded that ICP27 is a key regulator of PABP1 redistribution (6). We have also observed that the overexpression of ICP27 causes PABP1 nuclear relocation. However, it is clear from our experiments using ICP27-null mutant viruses that ICP27 is not necessary for the relocation of PABP1. Dobrikova et al. (6) reported that UL47 may also be implicated in PABP1 relocation. However, UL47 is a tegument protein that has roles early in virus infection at times when PABP relocation is not observed. Moreover, ICP27 transcriptionally regulates UL47 (22). This protein cannot contribute to PABP1 relocation, as it is not expressed at significant levels in cells infected with the 27lacZ or d27.1 virus. These data indicate that although ICP27 and PABP1 are found in the same complexes (10), ICP27 is not responsible for relocating PABP1 to the nucleus.

In HSV-1-infected cells there is an overall reduction in cellular mRNA levels due to virus inhibition of cellular transcription (47) and the degradation of cellular mRNAs. Early in infection, the *vhs* protein degrades all RNAs (46), and later in infection, ICP27 inhibits splicing, leading to an uncoupling of the RNA processing and RNA export pathways (14, 15, 45). Most viral mRNAs do not contain introns, so they are still efficiently exported to the cytoplasm (23). However, cellular mRNA export is significantly disrupted, and it seems likely that retained cellular mRNAs are degraded because fluorescence *in situ* hybridization confocal microscopy has demonstrated no net nuclear accumulation of polyadenylated RNA in HSV-1-infected cells (23). However, infection of cells with certain HSV-1 ICP27 mutant viruses can result in polyadenylated RNA accumulation in the nucleus (23). The ectopic overexpression of ICP27 could have an effect similar to that of these mutants by blocking cellular splicing and, therefore, mRNA export. Since PABP1 is known to bind pre-mRNAs in the nucleus (18), this raises the possibility that nuclear PABP1 may be associated with retained mRNAs.

The overexpression of PABP1 was previously shown to result in its accumulation in the nucleus (1); however, our data clearly establish that overall PABP1 levels are not increased during HSV-1 infection (Fig. 1C), and thus, this cannot account for our observations. The PABP1-paxillin interaction has been suggested to control levels of nuclear PABP1. HSV-1 infection seemed to disrupt this interaction, perhaps due to an altered phosphorylation of paxillin (57), which is observed during virus infection (Fig. 4B). Paxillin is known to be a target of JNK and p38 MAP kinase (19), both of which are activated during virus infection (Fig. 3A). However, it is clear that only a very small pool of PABP1 binds paxillin in uninfected cells, and the binding may be cell type specific, as we were unable to consistently detect a paxillin-PABP1 interaction in HeLa cells. Thus, the importance of the disruption of the paxillin-PABP1 interaction in HSV-1 infection may be low.

Virus binding and entry, replication, and protein translation all contribute to the induction of cellular stresses, including DNA damage (34), ER stress (37), oxidative stress (26), and apoptosis (39). Consistent with this, the stress-activated protein kinase pathways, particularly JNK and p38 MAPK, are activated during HSV-1 infection (16). Although mechanisms exist to reduce the stress-related disruption of the translation apparatus during HSV-1 infection (36), it is possible that PABP1 is evicted from the polyribosomes as a result of HSV-1-induced cell stress. Unlike in HSV-1 infected cells, the treatment of uninfected cells with many different exogenous stress inducers did not induce PABP1 relocation to the nucleus. However, the direct induction of oxidative stress resulted in a clear relocation of PABP1 to the nucleus. Hydrogen peroxide treatment mimicked the qualitative changes in selected JNK and MAP kinases activated during HSV-1 infection. In particular, JNK2 and p38α MAP kinase were activated by both types of cell stress. A direct causative link between HSV-1-induced oxidative stress and PABP1 nucleocytoplasmic localization remains to be established. However, although DNA damage induced by gamma irradiation did not induce PABP1 nuclear relocation, UV irradiation causes significant PABP1 entry into the nucleus (our unpublished data). Although UV irradiation causes DNA damage, it also induces oxidative stress. One effect of oxidative stress that we are currently investigating may be to inhibit the export of nuclear PABP1.

Many viruses have evolved mechanisms of disrupting PABP1 as a means of host cell shutoff. For example, the poliovirus 3C protease cleaves PABP1 on polyribosomes (29), and the rotavirus NSP3 protein competes with PABP1 for eIF4G binding (13). However, it remains to be determined

whether PABP1 relocalization in HSV-1 or KSHV (25, 33) plays a similar role. For instance, in HSV-1-infected cells, most cellular mRNAs are considered to be significantly depleted within the cytoplasm by late times, making additional PABP1-related shutoff mechanisms redundant. Indeed, PABP relocalization would be predicted to also impact efficient viral translation. To investigate whether PABP1 is required for the translation of HSV-1 late proteins, we depleted PABP1 levels in cells and then infected them with HSV-1. Total cellular PABP1 levels were very significantly decreased in our siRNA knockdown experiments, and cellular translation was reduced by almost 80%. Although it is possible that translation could tolerate very low levels of PABP1, steady-state levels of two cellular proteins were significantly reduced following PABP1 siRNA treatment, indicating that PABP1 knockdown could alter at least some cellular translation. Surprisingly, there was no obvious reduction in virus replication levels or in the production of selected steady-state virus proteins, including true late proteins, despite the efficient siRNA knockdown of PABP1 prior to virus infection. This means that the translation of virus proteins can tolerate very low levels of PABP1. This may be due to the lack of cellular mRNAs reducing competition for the translational apparatus. Consistent with this idea, human cytomegalovirus (HCMV), a herpesvirus that does not degrade cellular mRNAs, increases cellular levels of PABP and its recruitment into cap-binding complexes (2, 53, 56). Alternatively, HSV-1 may compensate for low levels of PABP1 on the polysomes by remodeling the translation apparatus to ensure efficient viral protein production (31). Several virus proteins, including ICP27, ICP6, and ICP0, have been implicated in the efficient assembly of the translation initiation complex (8, 9, 30, 55) and the phosphorylation of eIF4E, which regulates translation (54). It remains to be seen whether these proteins have a direct effect on translation during virus infection, perhaps to compensate for the loss of PABP1 on the polyribosomes.

REFERENCES

1. **Afonina, E., R. Stauber, and G. N. Pavlakis.** 1998. The human poly(A)-binding protein 1 shuttles between the nucleus and the cytoplasm. J. Biol. Chem. **273:**13015–13021.
2. **Arias, C., D. Walsh, J. Harbell, A. C. Wilson, and I. Mohr.** 2009. Activation of host translational control pathways by a viral developmental switch. PLoS Pathog. **5:**1–12.
3. **Beauchemin, C., and J.-F. Laliberté.** 2007. The poly(A) binding protein is internalized in virus-induced vesicles or redistributed to the nucleolus during turnip mosaic virus infection. J. Virol. **81:**10905–10913.
4. **Boutell, C., and R. D. Everett.** 2004. Herpes simplex virus type 1 infection induces the stabilization of p53 in a USP7- and ATM-independent manner. J. Virol. **78:**8068–8077.
5. **Deakin, N. O., and C. E. Turner.** 2008. Paxillin comes of age. J. Cell Sci. **121:**2435–2444.
6. **Dobrikova, E., M. Shveygert, R. Walters, and M. Gromeier.** 2010. Herpes simplex virus proteins ICP27 and UL47 associate with polyadenylate-binding protein and control its subcellular distribution. J. Virol. **84:**270–279.
7. **Dong, J.-M., L.-S. Lau, L. Lim, and E. Manser.** 2009. Paxillin nuclear-cytoplasmic localization is regulated by phosphorylation of the LD$_4$ motif: evidence that nuclear paxillin promotes cell proliferation. Biochem. J. **418:**173–184.
8. **Ellison, K. S., R. A. Maranchuk, K. L. Mottet, and J. R. Smiley.** 2005. Control of VP16 translation by the herpes simplex virus type 1 immediate-early protein ICP27. J. Virol. **79:**4120–4131.
9. **Fontaine-Rodriguez, E. C., and D. M. Knipe.** 2008. Herpes simplex virus ICP27 increases translation of a subset of viral late mRNAs. J. Virol. **82:**3538–3545.
10. **Fontaine-Rodriguez, E. C., T. J. Taylor, M. Olesky, and D. M. Knipe.** 2004. Proteomics of herpes simplex virus infected cell protein 27: association with translation initiation factors. Virology **330:**487–492.
11. **Gillis, P. A., L. H. Okagaki, and S. A. Rice.** 2009. Herpes simplex virus type 1 ICP27 induces p38 mitogen-activated protein kinase signaling and apoptosis in HeLa cells. J. Virol. **83:**1767–1777.
12. **Gorgoni, B., and N. K. Gray.** 2004. The roles of cytoplasmic poly(A)-binding proteins in regulating gene expression: a developmental perspective. Brief. Funct. Genomic. Proteomic. **3:**125–141.
13. **Harb, A., M. M. Becker, D. Vitour, C. H. Baron, P. Vende, S. C. Brown, S. Bolte, S. T. Arold, and D. Poncet.** 2008. Nuclear localization of cytoplasmic poly(A)-binding protein upon rotavirus infection involves the interaction of NSP3 with eIF4G and RoXaN. J. Virol. **82:**11283–11293.
14. **Hardwicke, M., and R. M. Sandri-Goldin.** 1994. The herpes simplex virus regulatory protein ICP27 contributes to the decrease in cellular mRNA levels during infection. J. Virol. **68:**4797–4810.
15. **Hardy, W. R., and R. M. Sandri-Goldin.** 1994. Herpes simplex virus inhibits host cell splicing and regulatory protein ICP27 is required for this effect. J. Virol. **68:**7790–7799.
16. **Hargett, D., T. McLean, and S. L. Bachenheimer.** 2005. Herpes simplex virus ICP27 activation of stress kinases JNK and p38. J. Virol. **79:**8348–8360.
17. **He, B., J. Choum, R. Brandimarti, I. Mohr, Y. Gluzman, and B. Roitzman.** 1997. Suppression of the phenotype of γ134.5⁻ herpes simplex virus 1: failure of activated RNA-dependent protein kinase to shut off protein synthesis is associated with a deletion in the domain of the α47 gene. J. Virol. **71:**6049–6054.
18. **Hosoda, N., F. Lejeune, and L. E. Maquat.** 2006. Evidence that poly(A)-binding protein C1 binds nuclear pre-mRNA poly(A) tails. Mol. Cell. Biol. **26:**3085–3097.
19. **Huang, C., K. Jacobson, and M. D. Schaller.** 2004. MAP kinases and cell migration. J. Cell Sci. **117:**4619–4628.
20. **Imataka, H., A. Gradi, and N. Sonenberg.** 1998. A newly defined N-terminal amino acid sequence of human eIF4G binds poly(A)-binding protein and functions in poly(A)-dependent translation. EMBO J. **17:**7480–7489.
21. **Jackson, R. J., C. U. T. Hellen, and T. V. Pestova.** 2010. The mechanism of eukaryotic translation initiation and principles of its regulation. Nat. Rev. Mol. Cell Biol. **10:**113–127.
22. **Jean, S., K. M. LeVan, B. Song, M. Levine, and D. M. Knipe.** 2010. Herpes simplex virus 1 ICP27 is required for transcription of two viral late (gamma2) genes in infected cells. Virology **283:**273–284.
23. **Johnson, L. A., and R. M. Sandri-Goldin.** 2009. Efficient nuclear export of herpes simplex virus 1 transcripts requires both RNA binding by ICP27 and ICP27 interaction with TAP/NXF1. J. Virol. **83:**1184–1192.
24. **Kahvejian, A., G. Roy, and N. Sonenberg.** 2001. The mRNA closed loop model: the function of PABP and PABP-interacting proteins in mRNA translation. Cold Spring Harbor Symp. Quant. Biol. **66:**300.
25. **Kanno, T., Y. Sato, T. Sata, and H. Katano.** 2006. Expression of Kaposi's sarcoma-associated herpesvirus-encoded K10/10.1 protein in tissues and its interaction with poly(A)-binding protein. Virology **352:**100–109.
26. **Kavouras, J. H., E. Prandovszky, K. Valyi-Nagy, S. K. Kovacs, V. Tiwari, M. Kovacs, D. Shukla, and T. Valyi-Nagy.** 2007. Herpes simplex virus type 1 infection induces oxidative stress and the release of bioactive lipid peroxidation by-products in mouse P19N neural cell cultures. J. Neurovirol. **13:**416–425.
27. **Khaleghpour, K., Y. V. Svitkin, A. W. Craig, C. T. DeMaria, R. C. Deo, S. K. Burley, and N. Sonenberg.** 2001. Translational repression by a novel partner of human poly(A) binding protein, Paip2. Mol. Cell **7:**205–216.
28. **Kuyumcu-Martinez, N. M., M. Joachims, and R. E. Lloyd.** 2002. Efficient cleavage of ribosome-associated poly(A) binding protein by enterovirus 3C protease. J. Virol. **76:**2062–2074.
29. **Kuyumcu-Martinez, N. M., M. E. Van Eden, P. Youan, and R. E. Lloyd.** 2004. Cleavage of poly(A)-binding protein by poliovirus 3C protease inhibits host cell translation: a novel mechanism for host translation shutoff. Mol. Cell. Biol. **24:**1779–1790.
30. **Larralde, O., R. W. P. Smith, G. S. Wilkie, P. Malik, N. K. Gray, and J. B. Clements.** 2006. Direct stimulation of translation by the multifunctional herpesvirus ICP27 protein. J. Virol. **80:**1588–1591.
31. **Laurent, A.-M., J.-J. Madjar, and A. Greco.** 1998. Translational control of viral and host protein synthesis during the course of herpes simplex virus type 1 infection: evidence that initiation of translation is the limiting step. J. Gen. Virol. **79:**2765–2775.
32. **Le, H., R. L. Tanguaym, M. L. Balasta, C. C. Wei, K. S. Browning, A. M. Metz, D. J. Goss, and D. R. Gallie.** 1997. Translation initiation factors

eIF-iso4G and eIF4B interact with the poly(A)-binding protein and increase its RNA binding activity. J. Biol. Chem. **272:**16247–16255.

33. **Lee, Y. J., and B. A. Glaunsinger.** 2009. Aberrant herpesvirus-induced poly-adenylation correlates with cellular messenger RNA destruction. PLoS Biol. **7:**e1000107.

34. **Lilley, C. E., C. T. Carson, A. R. Muotri, F. H. Gage, and M. D. Weitzman.** 2005. DNA repair proteins affect the lifecycle of herpes simplex virus 1. Proc. Natl. Acad. Sci. U. S. A. **102:**5844–5849.

35. **McCarthy, A. M., L. McMahan, and P. A. Schaffer.** 1989. Herpes simplex virus type 1 ICP27 deletion mutants exhibit altered patterns of transcription and are DNA deficient. J. Virol. **63:**18–27.

36. **Mulvey, M., C. Arias, and I. Mohr.** 2006. Resistance of mRNA translation to acute endoplasmic reticulum stress-inducing agents in herpes simplex virus type 1-infected cells requires multiple virus-encoded functions. J. Virol. **80:**7354–7363.

37. **Mulvey, M., C. Arias, and I. Mohr.** 2007. Maintenance of the endoplasmic reticulum (ER) homeostasis in herpes simplex virus type 1-infected cells through the association of a viral glycoprotein with PERK, a cellular ER stress sensor. J. Virol. **81:**3377–3390.

38. **Mulvey, M., J. Poppers, D. Sternberg, and I. Mohr.** 2003. Regulation of eIF2α phosphorylation by different functions that act during discrete phases in the herpes simplex virus type 1 life cycle. J. Virol. **77:**10917–10928.

39. **Nguyen, M. L., and J. A. Blaho.** 2007. Apoptosis during herpes simplex virus infection. Adv. Virus Res. **69:**67–97.

40. **Peters, G. A., D. Khoo, I. Mohr, and G. C. Sen.** 2002. Inhibition of PACT-mediated activation of PKR by the herpes simplex virus type 1 Us11 protein. J. Virol. **76:**11054–11064.

41. **Piron, M., P. Vende, J. Cohen, and D. Poncet.** 1998. Rotavirus RNA-binding protein NSP3 interacts with eIF4G1 and evicts the poly(A)-binding protein from eIF4F. EMBO J. **17:**5811–5821.

42. **Poppers, J., M. Mulvey, D. Khoo, and I. Mohr.** 2000. Inhibition of PKR activation by the proline-rich RNA binding domain of the herpes simplex virus type 1 US11 protein. J. Virol. **74:**11215–112221.

43. **Rice, S. A., and D. M. Knipe.** 1990. Genetic evidence for two distinct trans-activation functions of the herpes simplex virus alpha protein ICP27. J. Virol. **64:**1704–1715.

44. **Roizman, B., and D. M. Knipe.** 2001. Herpes simplex viruses and their replication, p. 2399–2459. *In* D. M. Knipe, P. M. Howley, D. E. Griffin, R. A. Lamb, M. A. Martin, B. Roizman, and S. E. Straus (ed.), Fields virology, 4th ed., vol. 2. Lippincott Williams & Wilkins, Philadelphia, PA.

45. **Sandri-Goldin, R. M., and G. E. Mendoza.** 1992. A herpesvirus regulatory protein appears to act post-transcriptionally by affecting mRNA processing. Genes Dev. **6:**848–863.

46. **Smiley, J. R.** 2004. Herpes simplex virus host shutoff protein: immune evasion by a viral RNase? J. Virol. **78:**1063–1068.

47. **Smiley, J. R., B. Panning, and C. A. Smibert.** 1991. Regulation of cellular genes by HSV products, p. 151–179. *In* E. K. Wagner (ed.), Herpesvirus transcription and its regulation. CRC Press, Boca Raton, FL.

48. **Smith, R. W. P., P. Malik, and J. B. Clements.** 2005. The herpes simplex virus ICP27 protein: a multifunctional post-transcriptional regulator of gene expression. Biochem. Soc. Trans. **33:**499–501.

49. **Smith, I. L., M. Hardwicke, and R. M. Sandri-Goldin.** 1992. Evidence that the herpes simplex virus immediate early protein ICP27 acts post-transcriptionally during infection to regulate gene expression. Virology **186:**74–86.

50. **Spriggs, K. A., M. Stoneley, M. Bushell, and A. E. Willis.** 2008. Re-programming of translation following cell stress allows IRES-mediated translation to predominate. Biol. Cell **100:**27–38.

51. **Tarun, S. Z., and A. B. Sachs.** 1996. Association of the yeast poly(A) binding protein with translation initiation factor eIF4G. EMBO J. **15:**7168–7177.

52. **van der Vlies, D., M. Makkinje, A. Jansens, I. Braakman, A. J. Verkleij, K. W. A. Wirtz, and J. A. Post.** 2004. Oxidation of ER resident proteins upon oxidative stress: effects of altering cellular redox/antioxidant status and implications for protein maturation. Antioxid. Redox Signal. **5:**381–389.

53. **Walsh, D., C. Arias, C. Perez, D. Halladin, M. Escandon, T. Ueda, R. Watanabe-Fukunaga, R. Fukunaga, and I. Mohr.** 2008. Eukaryotic translation initiation factor 4F architectural alterations accompany translation initiation factor redistribution in poxvirus-infected cells. Mol. Cell. Biol. **28:**2648–2658.

54. **Walsh, D., and I. Mohr.** 2004. Phosphorylation of eIF4E by Mnk-1 enhances HSV-1 translation and replication in quiescent cells. Genes Dev. **18:**660–672.

55. **Walsh, D., and I. Mohr.** 2006. Assembly of an active translation initiation factor complex by a viral protein. Genes Dev. **20:**461–472.

56. **Walsh, D., C. Perez, J. Notary, and I. Mohr.** 2005. Regulation of the translation initiation factor eIF4F by multiple mechanisms in human cytomegalovirus-infected cells. J. Virol. **79:**8057–8064.

57. **Woods, A. J., T. Kantidakis, H. Sabe, D. R. Critchley, and J. C. Norman.** 2005. Interaction of paxillin with poly(A)-binding protein 1 and its role in focal adhesion turnover and cell migration. Mol. Cell. Biol. **25:**3763–3773.

58. **Woods, A. J., M. S. Roberts, J. Choudhary, S. T. Barry, Y. MAzaki, H. Sabe, S. J. Morley, D. R. Critchley, and J. C. Norman.** 2002. Paxillin associates with poly(A)-binding protein 1 at the dense endoplasmic reticulum and the leading edge of migrating cells. J. Biol. Chem. **277:**6428–6437.

59. **Zachos, G., J. B. Clements, and J. Conner.** 1999. Herpes simplex virus type 1 infection stimulates p38/c-Jun N-terminal mitogen-activated protein kinase pathways and activates transcription factor AP-1. J. Biol. Chem. **274:**5097–5103.